Comparative Study of Prenatal Development Between *Myotis albescens* (Chiroptera: Vespertilionidae) and *Eumops patagonicus* (Chiroptera: Molossidae): The Chorionic Vesicle and Extraembryonic Membranes Considerations

FLORENCIA EVELYN RODRÍGUEZ,[1,2] **MARÍA TERESA SANDOVAL**,[1] **BLANCA BEATRIZ ÁLVAREZ**,[1] **AND DANIEL MARCELO LOMBARDO**[3]*

[1]Universidad Nacional del Nordeste, Facultad de Ciencias Exactas y Naturales y Agrimensura, Departamento de Biología, Avenida Libertad, Corrientes, Argentina
[2]Consejo Nacional de Investigaciones Científicas y Técnicas (CONICET), Argentina
[3]Universidad de Buenos Aires, Facultad de Ciencias Veterinarias, Instituto de Investigación y Tecnología en Reproducción Animal (INITRA), Cátedra de Histología y Embriología, Chorroain, Buenos Aires, Argentina

ABSTRACT

We presented a comparative study of two species of South American bats, *Myotis albescens* and *Eumops patagonicus*, about prenatal development. This study was carried out using 60 specimens, which were measured and photographed, and the embryonic stage was assigned by the staging system for *Carollia perspicillata*. We observed that the chorionic vesicle showed similarities in the disposition of the extraembryonic membranes, but they differed in characteristics of their yolk sac; in *E. patagonicus*, it was more glandular than *M. albescens*. *M. albescens* presented a well-developed discoid placenta with a caudal antimesometrial position, but *E. patagonicus* presented a diffuse placenta, which persists until the end of gestation and a discoid placenta in the uterus–tubal junction. In the embryogenesis, early stages, middle stages, and late stages were defined. In the early stage, the embryonic morphology is similar in the two species. The middle stage is characterized by the muzzle and pinna formation, fore and hind limb regionalization, and the formation of the patagium primordium. In the late stage, the overall growth of the embryo occurs. Its fore and hind limbs, patagium, and the typical craniofacial features are configured. We conclude that in early stages of development, the embryonic morphology of *M. albescens* and *E. patagonicus* is similar, while in late stages differences are evident; mainly the craniofacial structures and uropatagium configuration characteristics that allow their classification at the family level. Moreover, differences in time of fusion of maxillary and mandibular process were registered. This could be related to the morphology of the muzzle of each species. Anat Rec, 301:1527–1543, 2018. © 2018 Wiley Periodicals, Inc.

Grant sponsor: Secretaria General de Ciencia y Técnica de la Universidad Nacional del Nordeste; Grant number: PI: F12 008.

*Correspondence to: Lombardo Daniel Marcelo, Universidad de Buenos Aires, Facultad de Ciencias Veterinarias, Instituto de Investigación y Tecnología en Reproducción Animal (INITRA), Chorroain 280, Buenos Aires, Argentina. Fax: 54-11-528-72038.

E-mail: dlombard@fvet.uba.ar

Received 23 June 2017; Revised 2 February 2018; Accepted 14 February 2018.

DOI: 10.1002/ar.23896
Published online in Wiley Online Library (wileyonlinelibrary.com).

© 2018 WILEY PERIODICALS, INC.

Key words: South American bat; Chiroptera; Vespertilionidae; Molossidae; embryogenesis; chorionic vesicle

The order Chiroptera is the second largest order of mammals, including more than 1,100 species (Wilson and Reeder, 2005). It comprises two suborders Megachiroptera and Microchiroptera (Teeling et al., 2005) and 18 recognized families (Jones et al., 2002; Miller-Butterworth et al., 2007). Megachiroptera has reduced geographical distribution in tropical and subtropical regions of the Old World, Africa, Asia, Australia, and New Zealand. Whereas Microchiroptera is cosmopolitan, with representatives from almost every continent, including the majority of species, with over 900 species among 17 families (Nowak, 1999).

The knowledge about the embryonic development of Microchiroptera is restricted to a few species from North America such as *Myotis lucifugus* (Adams, 1992). There is a lack of knowledge about other species from Asia such as *Vespertilio murinus* (Schumacher, 1932), *Pipistrellus abramus* (Tokita, 2006), *Hipposideros armiger*, and *H. pratti* (Wang et al., 2010). There are other known species from Europe and Africa, such as *Miniopterus schreibersii fuliginosus* (Wang et al., 2010) and from Central and South America, such as *Carollia perspicillata* (Cretekos et al., 2005) and *Molossus rufus* (Nolte et al., 2009). The staging system proposed for *C. perspicillata* is, at present, the most complete and includes the embryo sequence from fertilization until the end of development. It systematizes a total of 24 embryonic stages and is used as a reference table. However, characteristics of chorionic vesicle have not been considered in previous studies. This information is important to interpret the maternal-embryonic relations during gestation.

The present study aimed to expand the knowledge about the ontogeny of the South American Chiroptera fauna and to contribute basic information and to carry out interspecific comparisons based on the staging system. The present study also aimed to characterize the embryonic development of *Myotis albacescens* (Vespertilionidae) and *Eumops patagonicus* (Molossidae), two central and South American species, belonging to two families of Microchiroptera, widely and commonly distributed in northern Argentina.

Myotis albescens is distributed in Central and South America (Fig. 1A,B). It is an insectivorous species of middle size (81.8–94 mm) with light gray pelage. In general, it has been associated with urban areas such as houses, buildings, crevices, rocks, etc. Mating is registered in May, with a possible delay in fertilization (Myers, 1977), and pregnant females appear at the end of July (Barquez et al., 1999).

E. patagonicus is distributed only in South America (Fig. 1C,D). It is an insectivorous species of middle to large size (99.2–120 mm), with gray-brown pelage. They live in urban and suburban areas. There is no information about mating, and pregnant females appear in September and October (Barquez et al., 1999).

In this study, we described and compared the chorionic vesicles and the disposition of the extraembryonic membranes of *M. albescens* and *E. patagonicus* in early, middle, and late embryonic stages. This information will be useful to carry out interspecific comparisons showing similarities and differences at the time of formation of the embryonic structures and would be useful as a model for studies related to heterochronic events.

MATERIALS AND METHODS

To obtain the embryos for this study, we analyzed 60 uteri from pregnant females of *M. albescens* (N = 28) and *E. patagonicus* (N = 32) in different stages of gestation. The pregnant females were captured manually during November 2009 and 2010, January 2010, and October 2014. The collection of samples took place in San Isidro (29°42′33″ S, 57°32′5″ W), San Lorenzo (28°8′14″ S, 58°46′3″ W) and Mercedes (29°11′5″ S, 58°4′25″ W), Corrientes, Argentina. These animals were sacrificed following the guidelines of American Veterinary Medical Association (2013) and the American Society of Mammalogy (Sikes et al., 2016).

The dissection was carried out in each animal to separate the reproductive tract. For each uterus, height and width were measured by a digital caliper of 0.01 precision. The uterine volume (UV) was calculated using spheroid's formula (Dunham, 1983). Then, each uterus was dissected for the analysis of the chorionic vesicle. The embryos and their extraembryonic membranes were also isolated. The embryos were colored with methylene blue, observed, and analyzed under a stereo microscope. The degree of translucency or opacity was considered as a measure of the cell mass density in the embryo. Relevant fact during ontogeny. All the embryos were measured at crown-rump length (CRL). From stage 17, the forearm length (FL) and hindlimb autopodium's length (HAL) were measured using a micrometric ocular mounted on a stereo microscope or with a digital caliper, depending on the embryos dimensions. External morphological characterization was carried out on each embryo, and they were assigned to an embryonic stage according to Cretekos et al. (2005). From these observations, drawings were made, and photographs were taken with a digital camera (Canon EOS REBEL T3i) mounted on a stereomicroscope Leica EZ4.

RESULTS

Morphology of Uterus and Chorionic Vesicle

In *M. albescens*, the uterus is bicornuate with short horns, and the implantation is unilateral, that is, in the right horn. During gestation, the right horn becomes bigger than the left one, and adopts an oblong shape, while the left horn is relegated to the caudal position. The chorionic vesicle (Fig. 2) is unique and covered the entire uterine cavity, and its volume varies between 74 and 800.8 mm^3, depending on the stage of gestation (Table 1). The uterine cavity is internally lined by smooth chorion, with a placental disc in the antimesometrial position. The embryo is completely covered by the amniotic membrane, except in stage 12. The yolk sac is oval, irregular, and has thin walls that are highly vascularized and translucent.

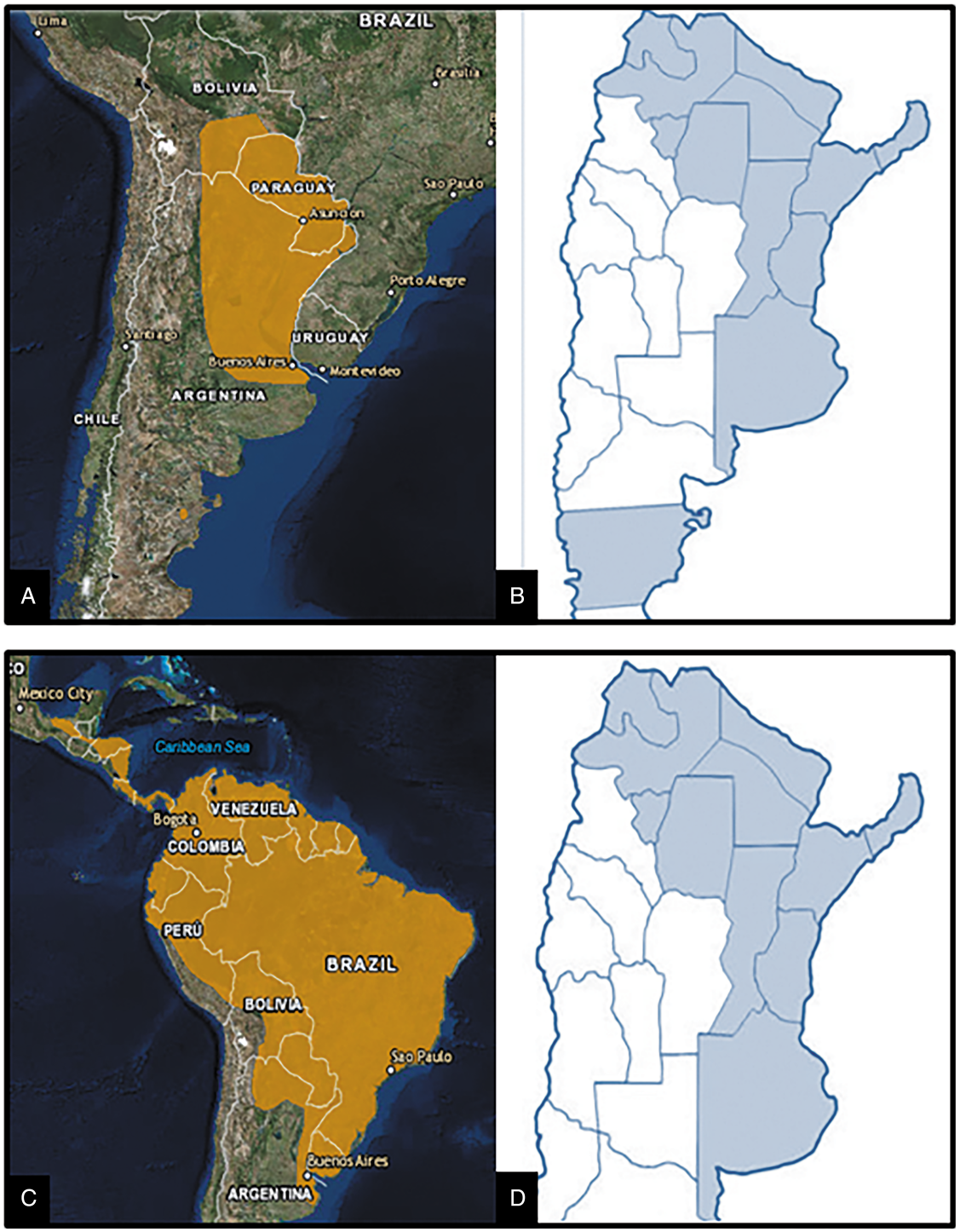

Fig. 1. Global distribution and Argentinian distribution. (**A**) Global distribution of *Myotis albescens*, (**B**) Argentinian distribution of *M. albescens*, (**C**) global distribution of *Eumops patagonicus*, and (**D**) Argentinian distribution of *E. patagonicus* (Barquez et al., 1999).

It is smaller than the embryo and located on the left flank of it, compressed between the amniotic membrane and the chorion.

In *E. patagonicus*, the uterus is bicornuate with short horns, and the implantation is unilateral, that is, in the right horn. During gestation, the right horn becomes large and adopts a rounded shape, while the other horn is reduced, staying in the lateral and caudal position. The chorionic vesicle (Fig. 3) is unique, rounded in shape, and occupies the entire horn; its volume varies between 214.5 and 3440.62 mm^3, depending on the stage of gestation (Table 1). The uterine cavity is internally lined by

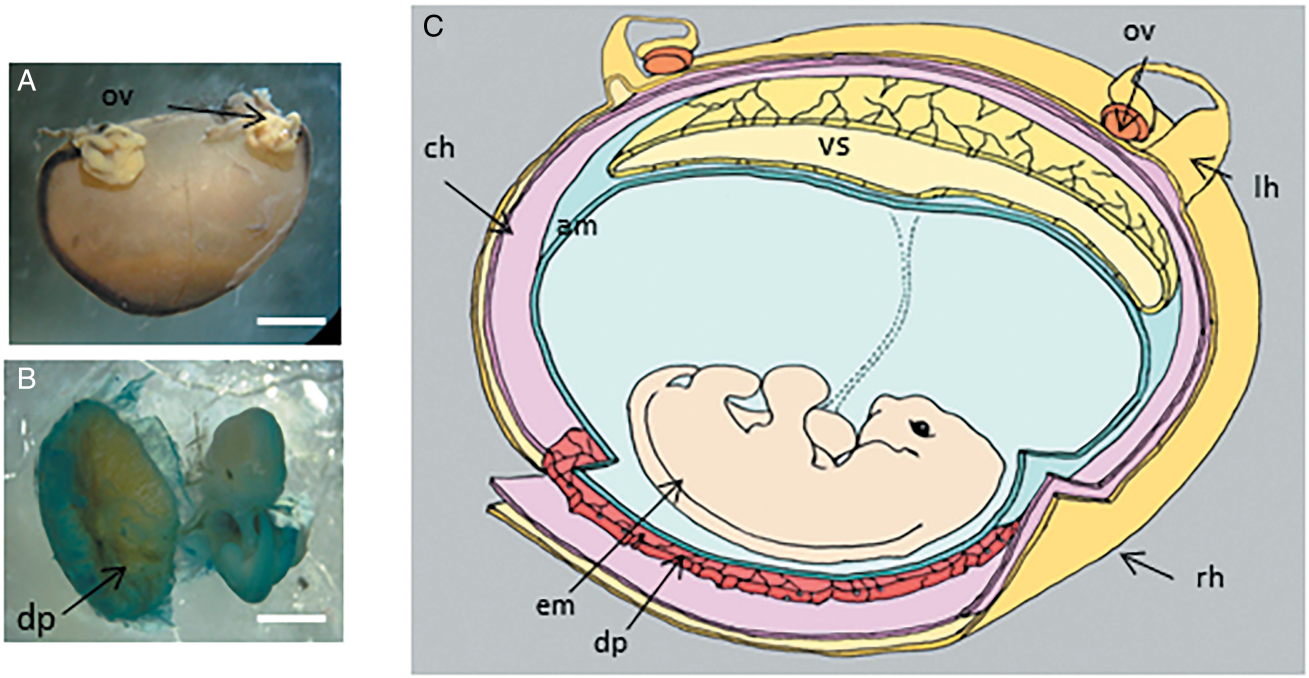

Fig. 2. Uterus and chorionic vesicle of *Myotis albescens* at the middle stage of gestation. (**A**) External view of the uterus, (**B**) embryo with the discoidal placenta, and (**C**) diagram of a uterus containing an embryo with extra-embryonic membranes. Abbreviations: am, amnion; ch, chorion; dp, discoidal placenta; em, embryo; lh, left horn; ov, ovary; rh, right horn; *vs*, vitelline sack. Scale bar = 2 mm.

rudimentary chorionic villi, with a small placental disc in the uterus tubal junction, whose size increases during gestation. The yolk sac is rounded in shape and laterally compressed, with thick walls, which are highly vascularized. It is pale yellow and opaque and is located toward the left side of the embryo. Its size is variable during gestation and is similar to the size of the embryo.

STAGES OF EMBRYONIC DEVELOPMENT BY CRETEKOS ET AL. (2005)

M. albescens (Figs. 4 and 5)

Stage 12. CRL: 2.49 mm (N = 1) (Fig. 4A–C). The embryo is translucent, with a "C" shape. The body is divided into three parts: the head, trunk, and tail. The cervical flexure is evident. The stomodeum invagination, the optic vesicle, and the otic vesicle are visible. The pharyngeal arch I and II are very clear. The heart has a prominent atrial and ventricular chamber. The primordium of the forearm is visible. The tail is flexed to the right.

Stage 14. CRL: 5.14 mm (N = 1) (Fig. 4D–G). The embryo is opaque and whitish, with a "C" shape. The midbrain is prominent, and cervical flexure is still evident. Eyes are oval in shape and pigmentation of the retina can be observed. The maxillary process exceeds the ocular region. The prominent mandibular process is not fused in the midline. Nasal processes without fusion and auditory hillocks are visible, surrounding the first pharyngeal arch. The lateral body wall is not fused in the midline. The forelimb is organized in the proximal–distal region; the digital plate is formed at the distal part of the forelimb. The hindlimb is digitiform—without regionalization. The plagiopatagium primordium is visible in the axillary region of the forelimb. The tail is free.

Stage 15. CRL: 6.07 ± 0.44 mm (N = 2) (Fig. 4H–K). The embryo is opaque and whitish. The maxillary processes are fused together in the midline and are fused with the nasal processes. Mandibular processes are fused together in the midline. In the eyes, the retina is more pigmented than in the previous stage. The auditory meatus is visible; auricle prominences are differentiated in helix, tragus, and antitragus. The lateral body wall is fused in the midline to the cardiac region. Prominent autopodium of the forelimb is flat and triangular with projections of digits 1 and 5. The hindlimb is differentiated in the proximal-distal region. The plagiopatagium fold is extended to the hindlimb. The tail is free.

Stage 16. CRL: 6.56 ± 0.57 mm (N = 3) (Fig. 4L–O). The embryo is opaque and whitish. The muzzle is well defined. Whisker follicles are visible in the side region of the upper jaw. Eyelid primordium is visible, and the helix, tragus, and antitragus are larger than in the previous stage. The lateral body wall is completely fused in the midline, except in the umbilical region. Forelimbs and hindlimbs are similar to those of the previous stage. The propatagium primordium is visible; the plagiopatagium extends from the base of the autopodium of the forelimb until the proximal region of the hindlimb. The uropatagium primordium is visible. The tail is free.

Stage 17. CRL: 7.68 ± 0.47 mm (N = 12) (Fig. 5A–D). The embryo is opaque and whitish. The muzzle is well defined. The whisker follicles are more developed than in

TABLE 1. Summary of *Myotis albescens* and *Eumops patagonicus* characteristics of staging system

	Myotis albescens					*Eumops patagonicus*				
Stage	Key features	UV (mm^3)	CRL (mm)	FL (mm)	HAL (mm)	Key features	UV (mm^3)	CRL (mm)	FL (mm)	HAL (mm)
12	The body is differentiated in the head, trunk, and tail. The optic vesicle and the otic vesicle are visible. The pharyngeal arch I and II are well evident. Forelimb buds.	73.91 N = 1	2.49	–	–	–	–	–	–	–
13	–			–	–	The body is differentiated in the head, trunk, and tail. Stomodeum. The optic vesicle and the otic vesicle are visible. The first arch is divided into maxillary and mandibular processes. Hindlimb bud and forelimb bud.	214.52 ± 94.06 N = 2	4.52 ± 0.84	–	–
14	Midbrain prominent. The retina is pigmented. Auditory hillocks are visible. Forelimb organized in a proximal–distal region. The hindlimb is digitiform. The plagiopatagium primordium is visible in the axillary region. The tail is free.	189.43 N = 1	5.14	–	–	Midbrain prominent. The retina is pigmented. Auditory hillocks are visible. Forelimb organized in a proximal–distal region. The hindlimb is digitiform. The plagiopatagium primordium is visible in the axillary region. The tail is free.	275.67 N = 1	5.76	–	–
15	The maxillary processes are fused together in the midline and with the nasal processes. Mandibular processes are fused. The auditory meatus is visible; auricle prominences are differentiated in helix, tragus, and antitragus. Prominent autopodium of the forelimb, flat triangular.	304.00 ± 17.48 N = 2	6.07 ± 0.44	–	–	The maxillary process, mandibular process, and nasal process are more developed than in the previous stage. Auricle prominences are differentiated in helix, tragus, and antitragus. Prominent autopodium of the forelimb, flat triangular.	251.17 ± 112.85 N = 2	6.8 ± 0.33	–	–
16	The muzzle is well defined. Whisker follicles are visible in the side region of the upper jaw. Eyelid primordium is visible. The propatagium primordium is visible. The tail is free.	284.47 ± 81.16 N = 3	6.56 ± 0.57	–	–	The maxillary processes are fused to each other and with the nasal process. Eyelid primordium is visible. The auditory meatus is visible The propatagium primordium is visible. The plagiopatagium is visible. The tail is free.	455.51 ± 61.65 N = 7	7.34 ± 0.52	–	–

(Continues)

TABLE 1. Continued

	Myotis albescens					*Eumops patagonicus*				
Stage	Key features	UV (mm^3)	CRL (mm)	FL (mm)	HAL (mm)	Key features	UV (mm^3)	CRL (mm)	FL (mm)	HAL (mm)
17	The mouth opens with the tongue visible. Helix is triangular, with its folded corner. Forelimb is morphologically distinguished in stylopodium, zeugopodium and autopodium, digits 2–5 are and linked to each other by the chiropatagium. The tail is free.	409.29 ± 71.38 N = 12	7.68 ± 0.47	1.42 ± 0.18	1.03 ± 0.13	The muzzle is well defined. The whisker follicles are visible. Helix with dorsal ridge that extends to the eye region. Forelimb is morphologically distinguished in stylopodium, zeugopodium and autopodium, digits 2–5 are and linked to each other by the chiropatagium. The distal region of the tail is free.	626.82 ± 98.27 N = 3	9.3 ± 0.57	1.66 ± 0.49	1.28 ± 0.28
18	The eyelids cover half of the eye. The digit 1 (thumb) of the wing is free. The digits of the hindlimb are free and similar in length.	549.59 ± 79.8 N = 4	9.09 ± 0.61	2.57 ± 0.70	1.40 ± 0.13	The eyelids cover half of the eye. The dorsal ridge of the helix extended to the frontal region and fused with the other side. The digit 1 (thumb) of the wing is free. The digits of the hindlimb are free and similar in length.	1057.03 ± 243.82 N = 2	11.3 ± 0.20	3.02 ± 0.59	1.83 ± 0.13
19	The eyelids cover the eyes. The helix is obliterated the meatus and the tragus. Patagium is translucent. The thumb of the forelimb and digits 1–5 of the hindlimb have a claw primordium. The tail is included in the uropatagium.	560.95 ± 106.18 N = 3	9.34 ± 0.38	2.66 ± 0.38	1.43 ± 0.04	The helix is more developed than in the previous stage and extends, covering the eyes completely. Tragus and antitragus are flat. The eyelids are closed. The thumb of the forelimb and digits 1–5 of the hindlimb have a claw primordium. The distal region of the tail is free.	1089.88 ± 217.08 N = 3	11.68 ± 0.70	3.55 ± 0.28	1.9 ± 0.15
20	Integument of the body with visible hair follicles. The calcaneus is visible, and the tail is similar than in the previous stage.	800.76 ± 221.74 N = 2	10.46 ± 0.28	3.57 ± 0.05	1.85 ± 0.03	Integument of the body with visible hair follicles. The calcaneus is visible, and the tail is similar than in the previous stage.	1197.73 ± 298.45 N = 2	13.6 ± 0.41	4.56 ± 0.67	2.44 ± 0.09
21	–					Helix highly developed, forming two large expansions that cover the ocular region muzzle is well developed, flange of rhinarium is visible.	1340.79 N = 1	13.9	4.27	2.39

(Continues)

TABLE 1. Continued

	Myotis albescens					*Eumops patagonicus*				
Stage	Key features	UV (mm^3)	CRL (mm)	FL (mm)	HAL (mm)	Key features	UV (mm^3)	CRL (mm)	FL (mm)	HAL (mm)
22	–					The eyelids are not fussed. The rhinarium is prominent, and the muzzle is more developed and with brown pigment spots in the maxillary region. The external genitals are well developed.	2808.76 ± 1006.45 N = 3	18.62 ± 0.64	10.37 ± 2.1	4.78 ± 1.18
23	–					The trunk of light brown coloration with pigments dispersed points.	2909.28 ± 673.54 N = 3	17.18 ± 0.69	10.38 ± 0.90	5.29 ± 1.13
24	–					The wing does not have pigment in the membranes; the patagios are translucent. The genitalia is well developed and pigmented.	3440.6 ± 37.69 N = 2	20.13 ± 0.84	12.93 ± 0.43	6.37 ± 0.69
25						Vibrissae and hairs are visible in upper and lower jaw. The eyelids are opens. There is hair in the hindlimb autopodium.	4547.7 N = 1	29.79	14.52	6.68

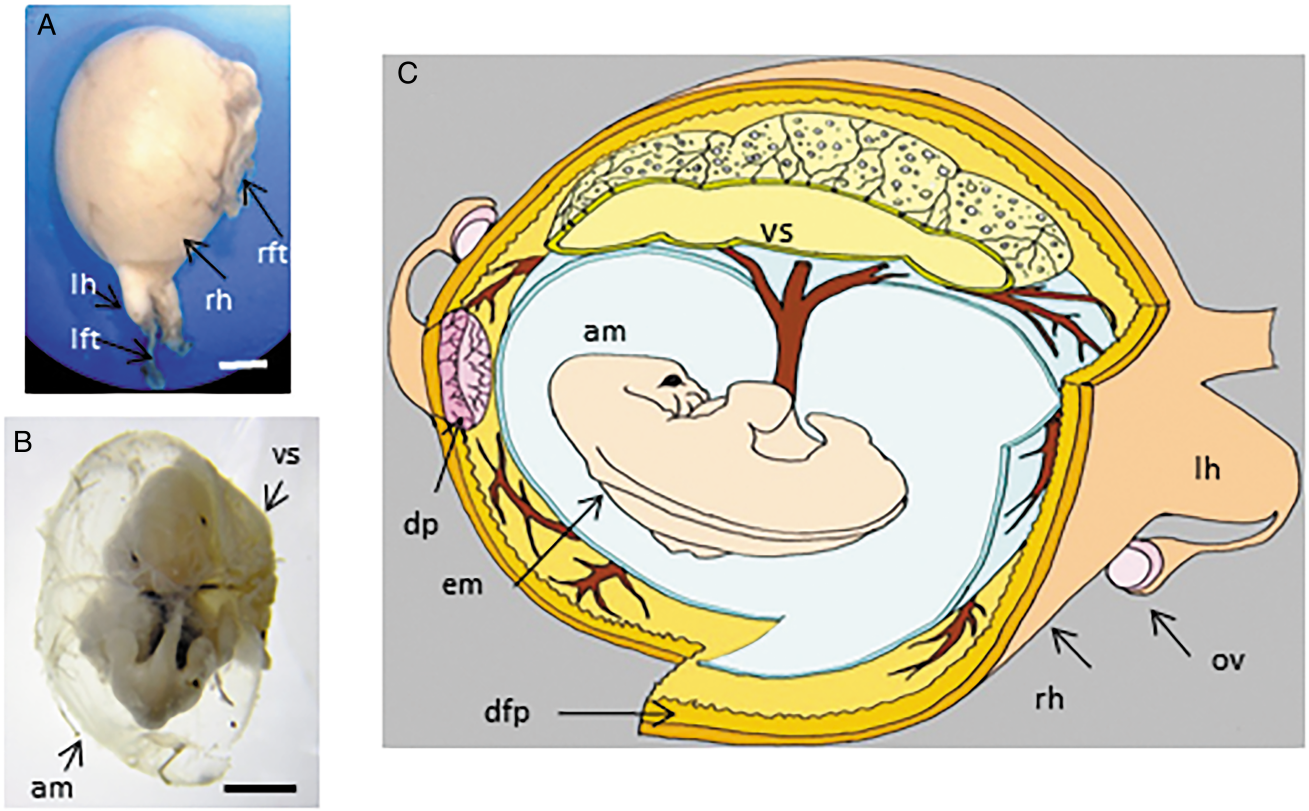

Fig. 3. Uterus and chorionic vesicle of *Eumops patagonicus* at the middle stage of gestation. (**A**) External view of the uterus, (**B**) embryo with amnion and vitelline sack, and (**C**) diagram of a uterus containing an embryo with extra-embryonic membranes. Abbreviations: am, amnion; ch, chorion; dp, discoidal placenta; dfp, diffuse placenta; em, embryo; lh, left horn; lft, left fallopian tube; ov, ovary; rh, right horn; rft, right fallopian tube; *vs*, vitelline sack. Scale bar = 2 mm.

the previous stage. The mouth opens with the tongue visible. The eyelids are similar to those in the previous stage. The helix is triangular and is more developed than in the previous stage, with its corner folded. The tragus is similar to that of the previous stage. The lateral body wall is opaque. The propatagium extends from the base of the stylopodium to the carpal region. The plagiopatagium extends to knees. The uropatagium extends from the base of the autopodium to the base of the tail. The forelimb is morphologically distinguished in the stylopodium, the zeugopodium, and the autopodium, with digits 1 and 2 more developed than in the previous stage, and the digits 2, 3, and 4 are visible and linked to each other by the chiropatagium. The knee and elbow are recognized as pronounced flexures. The hindlimb, with the stylopodium and the zeugopodium, is separated by the knee flexion. The digits are visible, of similar length and the interdigital membrane links them. The tail is free.

Stage 18. CRL: 9.09 ± 0.61 mm (N = 4) (Fig. 5E–H). The embryo is opaque and whitish. The muzzle is well developed and prominent. The eyelids cover half of the eye. The helix is more developed than in the previous stage and plicate, so it blocks the meatus and the tragus. The propatagium and the plagiopatagium are more developed than in the previous stage. The plagiopatagium extends from the digit 5 of the forelimb to the base of the autopodium of the hindlimb. The uropatagium extends to half of the tail. The autopodium of the forelimb is supported on the snout, covering the ocular region. The digit 1 (thumb) is free; digits 2–5 are longer than in the previous stage and linked by the chiropatagium. The digits of the hindlimb are free and similar in length. The distal region of the tail is free.

Stage 19. CRL: 9.34 ± 0.38 mm (N = 3) (Fig. 5I–L). The embryo is opaque and whitish. The eyelids cover the eyes. The helix is more developed and plicate than in the previous stage, covering the meatus and the tragus. The propatagium and the plagiopatagium are more developed than in the previous stages and translucent. The uropatagium extends to the end of the tail. The stylopodium, zeugopodium, and phalanges of the forelimb and hindlimb are more developed than the preceding stage. The chiropatagium is translucent. The thumb of the forelimb and digits 1–5 of the hindlimb have a primordium claw. The autopodium of the forelimb covers the muzzle region. The tail is included in the uropatagium.

Stage 20. CRL: 10.46 ± 0.28 mm (N = 2) (Fig. 5M–P). The embryo is opaque and whitish. The cephalic region is similar to in the previous stage. The integument of the body has visible hair follicles. The forelimb, hindlimb, and claws are more developed than in the preceding stage. The calcaneus is visible, and the tail is similar to in the previous stage.

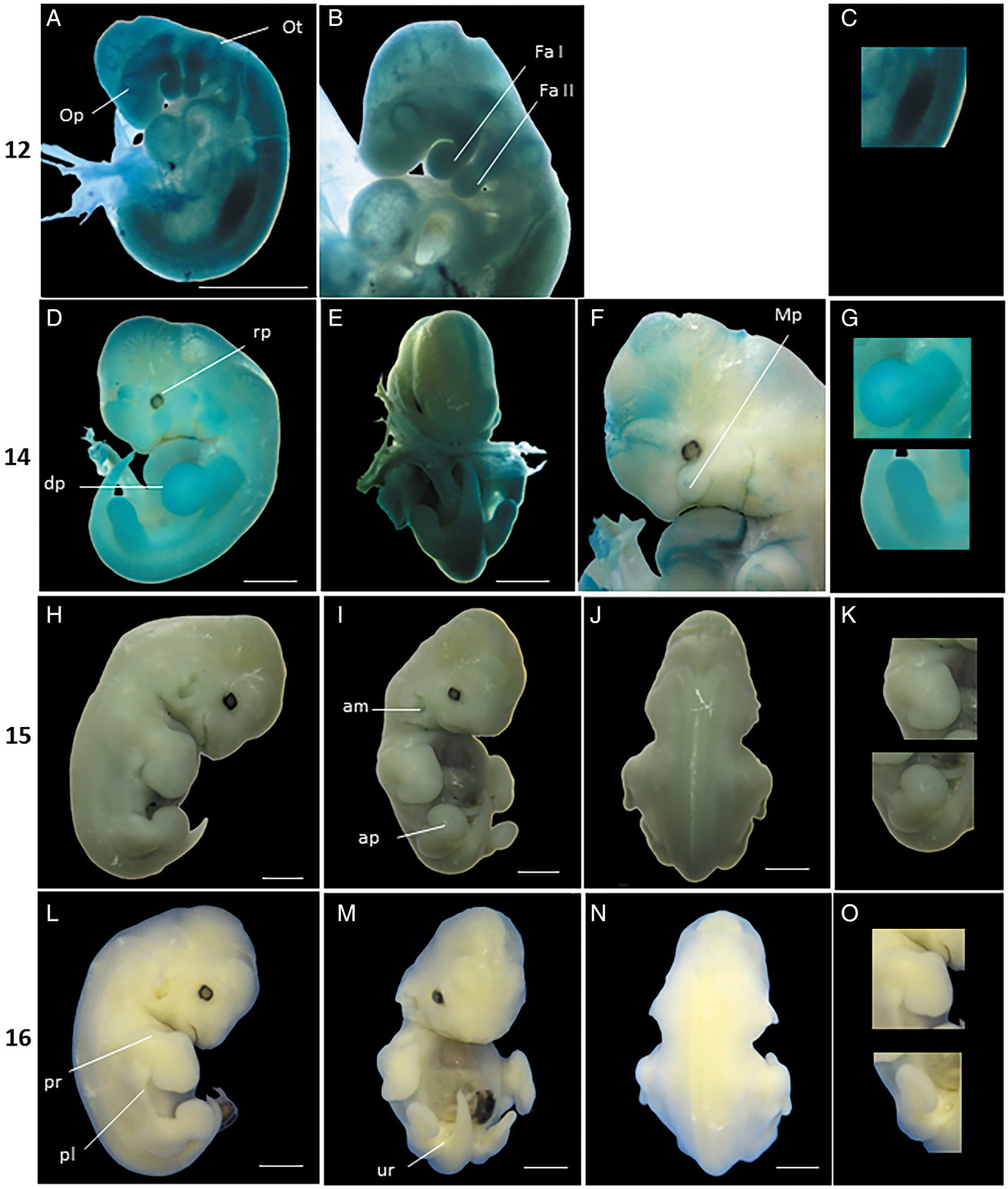

Fig. 4. *Myotis albescens* at embryonic stages 12–16. Stage 12, (**A**) lateral view from left side, (**B**) craniofacial view, (**C**) close-up for the forelimb bud. Stage 14, (**D**) lateral view from left side, (**E**) ventral view, (**F**) craniofacial view, and (**G**) close-up for the forelimb bud and hindlimb bud. Stage 15, (**H**) lateral view, (**I**) ventral view, (**J**) dorsal view, and (**K**) close-up for the forelimb bud and hindlimb bud. Stage 16, (**L**) lateral view, (**M**) ventral view, (**N**) dorsal view, and (**O**) close-up for the forelimb bud and hindlimb bud. Abbreviations: Am, auditori meatus; au, autopodium; dp, digital plate; fa I, pharyngeal arch I; fa II, pharyngeal archII; mp, maxillary process; op, optic vesicle; ot, otic vesicle; pl, plagiopatagium; pr, propatagium; rp, pigmented retina; ur, uropatagium. Scale bar = 1 mm.

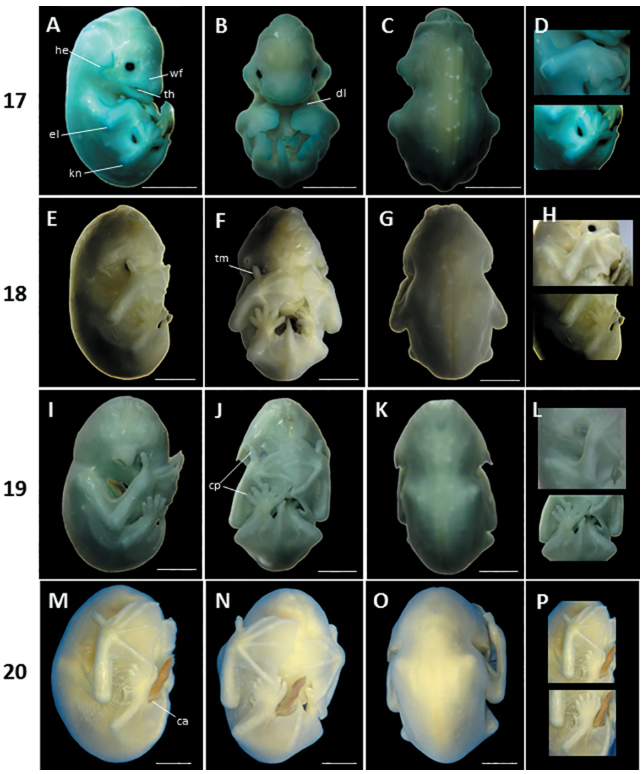

Fig. 5. *Myotis albescens* at embryonic stages 17–20. Stage 17, (**A**) lateral view, (**B**) ventral view, (**C**) dorsal view, and (**D**) close-up for the hindlimb and forelimb. Stage 18, (**E**) lateral view, (**F**) ventral view, (**G**) dorsal view, (**H**) close-up for the forelimb bud and hindlimb bud, Stage 19, (**I**) lateral view, (**J**) ventral view, (**K**) dorsal view, and (**L**) close-up for the forelimb bud and hindlimb bud. Stage 20, (**M**) lateral view, (**N**) ventral view, (**O**) dorsal view, and (**P**) close-up for the forelimb bud and hindlimb bud. Abbreviations: ca, calcaneus; cp, claw primordium; dl, digit I; el, elbow; kn, knee; th, tongue; tm, thumb; wf, whisker follicles. Scale bar = 1 mm.

E. patagonicus (Figs. 6–8)

Stage 13. CRL: 4.52 ± 0.84 mm (N = 2) (Fig. 6A–D). The embryo is opaque and with a "C" shape. The body is divided into three parts: head, trunk, and tail. The cervical flexure is evident. The stomodeum invagination, the optic vesicle, and the otic vesicle are visible. The pharyngeal arch I and II are evident. The first arch is divided into maxillary and mandibular processes, and the nasal process is evident. The lateral body wall is not fused in the midline. Digitiform hindlimb buds and forelimb buds are evident. The cardiac region is prominent. The tail is well developed.

Stage 14. CRL: 5.76 mm (N = 1) (Fig. 6E–H). The embryo is opaque and whitish with a "C" shape. The midbrain is prominent; the cervical flexure is still evident, eyes are oval in shape, and pigmentation of the retina can be observed. The maxillary process exceeds the ocular region. The mandibular process is not fused in the midline, and the nasal process is not fused. The auditory hillock surrounds the first pharyngeal arch. The lateral body wall is not fused in the midline. The forelimb is divided into the proximal and distal regions, and the hindlimb is digitiform, without regionalization. The primordium of the plagiopatagium is visible in the axillary region of the forelimb. The tail is free and longer than in the previous species.

Stage 15. CRL: 6.8 ± 0.33 mm (N = 2) (Fig. 6I–L). The embryo is opaque and whitish. The maxillary process, mandibular process, and nasal process are more developed than in the previous stage. In the eyes, the retina is more pigmented than in the previous stage. Auricle prominences are divided into the helix, tragus, and antitragus. The lateral body wall is fused in the midline to the hepatic region. Prominent forelimb autopodium is visible, and is triangular, with projections of digits 1 and 5. The hindlimb is divided into the proximal and distal region. The plagiopatagium primordium is extended to the hindlimb. The tail is free.

Stage 16. CRL: 7.34 ± 0.52 mm (N = 7) (Fig. 6M–P). The embryo is opaque and whitish. The maxillary processes are fused to each other and with the nasal process in the midline. Mandibular processes are fused together in the midline. The eyelid primordium is visible. The auditory meatus is visible. The helix, tragus, and antitragus are bigger than in the previous stage. The lateral body wall is fused in the midline, except in the umbilical region. The forelimbs and hindlimbs are similar to those of the previous stage. The propatagium primordium is visible. The plagiopatagium extends from the base of the autopodium of the forelimb to the proximal region of the hindlimb. The uropatagium primordium is visible. The tail is free.

Stage 17. CRL: 9.3 ± 0.57 mm (N = 3) (Fig. 6Q–T). The embryo is opaque and whitish. The muzzle is well defined. The whisker follicles are visible as slight bumps on the lateral surface of the upper jaw. The eyelid is similar to in the previous stage. The nasal wings are visible. The helix is more developed than in the previous stages and with a dorsal ridge that extends to the eye region. The tragus and antitragus are longer than previous stages. The propatagium extends from the base of the stylopodium to the carpal region. The plagiopatagium extends to the knees. The uropatagium extends from the base of the autopodium to the base of the tail. The forelimb is morphologically divided into the stylopodium, zeugopodium, and autopodium with digits 1 and 2 more developed than in the previous stage, and the digits 2, 3, and 4 are visible and linked to each other by the chiropatagium. The knee and elbow are recognized as pronounced flexures. The knee flexion separates the hindlimb into the stylopodium and zeugopodium. The digits are visible and of similar length, and the interdigital membrane links them. The distal region of the tail is free.

Stage 18. CRL: 11.3 ± 0.20 mm (N = 2) (Fig. 7A–D). The embryo is opaque and whitish. The muzzle is well developed and prominent. The eyelids cover half of the eye. The dorsal ridge of the helix extends to the frontal region and is fused with the other side, covering the middle of the eye. The propatagium is more developed than in the previous stage. The plagiopatagium is more developed and extends from the digit 5 of the forelimb to the base of the hindlimb autopodium. The uropatagium

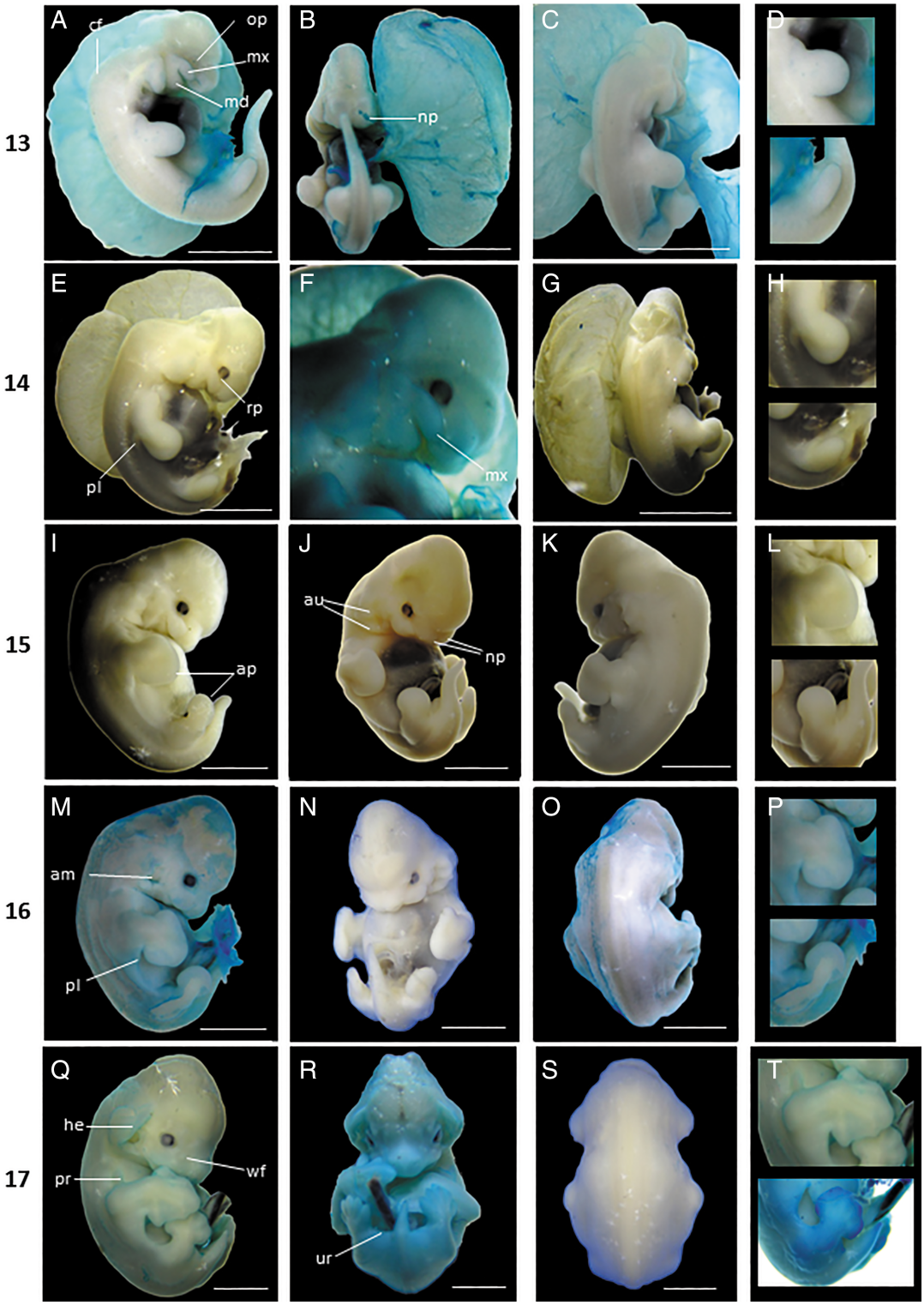

Fig. 6. *Eumops patagonicus* at embryonic stages 13–16. Stage 13, (**A**) lateral view, (**B**) ventral view, (**C**) dorsal view, and (**D**) close-up for the hindlimb and forelimb. Stage 14, (**E**) lateral view, (**F**) ventral view, (**G**) dorsal view, (**H**) close-up for the forelimb bud and hindlimb bud, Stage 15, (**I**) lateral view, (**J**) ventral view, (**K**) dorsal view, and (**L**) close-up for the forelimb bud and hindlimb bud. Stage 16, (**M**) lateral view, (**N**) ventral view, (**O**) dorsal view, and (**P**) close-up for the forelimb bud and hindlimb bud. Stage 17, (**Q**) lateral view, (**R**) ventral view, (**S**) dorsal view, and (**T**) close-up for the hindlimb and forelimb. Abbreviations: Am, auditory meatus; ap, autopodium; au, auricle primordium; *cf*, cervical flexure; he, helix; md, mandibubular process; mx, maxillary process; np, nasal process; op, optic vesicle; pl, plagiopatagium; pr, propatagium; rp, retina pigmented; ur, uropatagium; wf, whisker follicles. Scale bar = 2 mm.

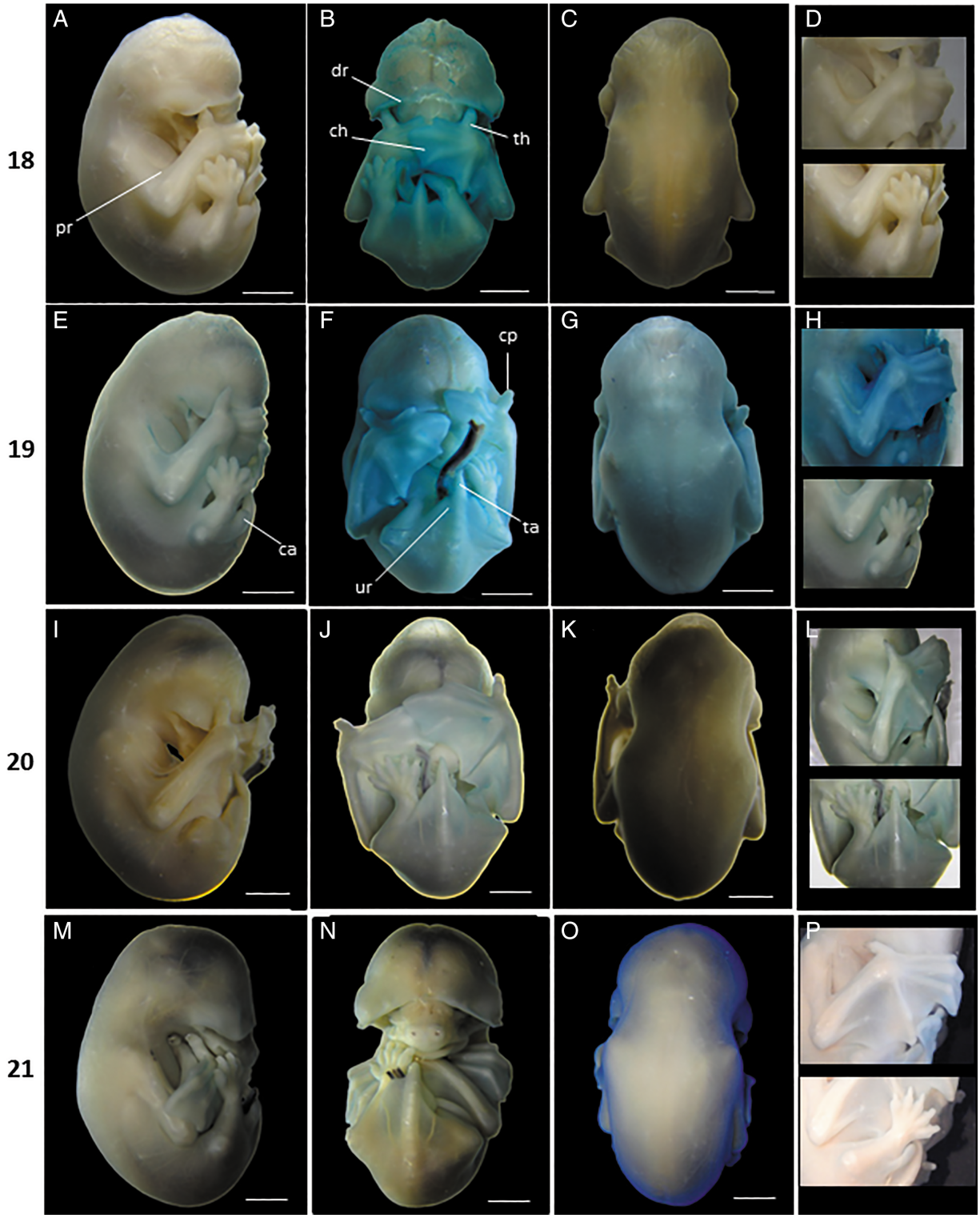

Fig. 7. *Eumops patagonicus* at embryonic stages 18–21. Stage 18, (**A**) lateral view, (**B**) ventral view, (**C**) dorsal view, and (**D**) close-up for the forelimb bud and hindlimb bud. Stage 19, (**E**) lateral view, (**F**) ventral view, (**G**) dorsal view, and (**H**) close-up for the forelimb bud and hindlimb bud. Stage 20, (**I**) lateral view, (**J**) ventral view, (**K**) dorsal view, and (**L**) close-up for the forelimb bud and hindlimb bud. Stage 21, (**M**) lateral view, (**N**) ventral view, (**O**) dorsal view, and (**P**) close-up for the hindlimb and forelimb. Scale bar = 2 mm. Fig. 8 *Eumops patagonicus* at embryonic stages 22–25. Stage 22, (**A**) lateral view, (**B**) ventral view, (**C**) dorsal view, and (**D**) close-up for the forelimb bud and hindlimb bud, Stage 23, (**E**) lateral view, (**F**) ventral view, (**G**) dorsal view, and (**H**) close-up for the forelimb bud and hindlimb bud. Stage 24, (**I**) lateral view, (**J**) ventral view, (**K**) dorsal view, and (**L**) close-up for the forelimb bud and hindlimb bud. Stage 25, (**M**) Lateral view, (**N**) ventral view, (**O**) dorsal view, and (**P**) close-up for the forelimb bud and hindlimb bud. Abbreviations: Ca, calcaneus; ch, chiropatagium; cl, claw; dr, dorsal ridge of the helix; pr, propatagium; ta, tail; th, thumb; ur, uropatagium. Scale bar = 2 mm.

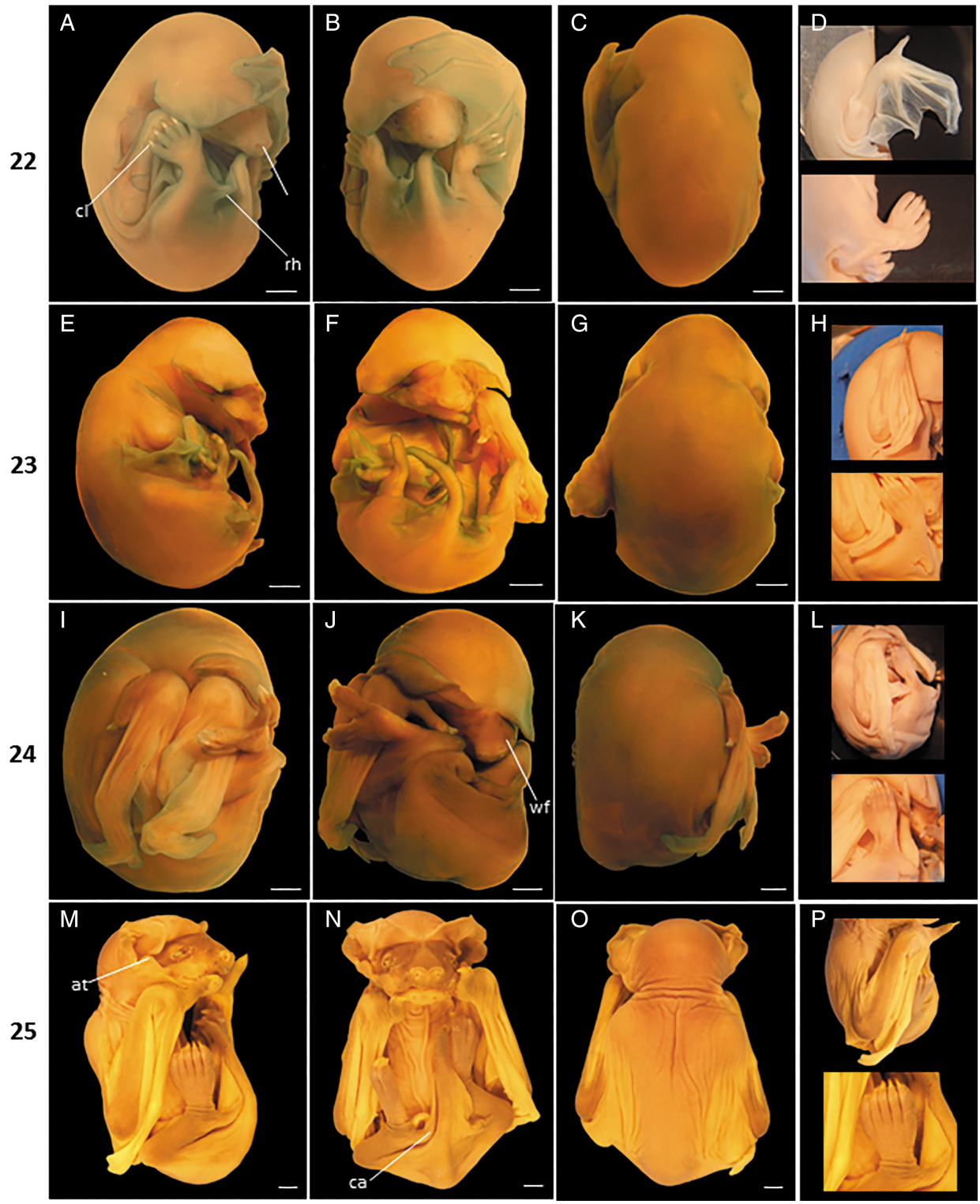

Fig. 8. *Eumops patagonicus* at embryonic stages 22–25. Stage 22, (**A**) lateral view, (**B**) ventral view, (**C**) dorsal view, and (**D**) close-up for the forelimb bud and hindlimb bud. Stage 23, (**E**) lateral view, (**F**) ventral view, (**G**) dorsal view, and (**H**) close-up for the forelimb bud and hindlimb bud. Stage 24, (**I**) lateral view, (**J**) ventral view, (**K**) dorsal view, (**L**) cose-up for the forelimb bud and hindlimb bud.Stage 25, (**M**) Lateral view, (**N**) ventral view, (**O**) dorsal view, and (**P**) close-up for the forelimb bud and hindlimb bud. Abbreviations: At, antitragus; ca, calcaneus; cl, claw; rh, rhinarium; wf, whisker follicles. Scale bar = 2 mm.

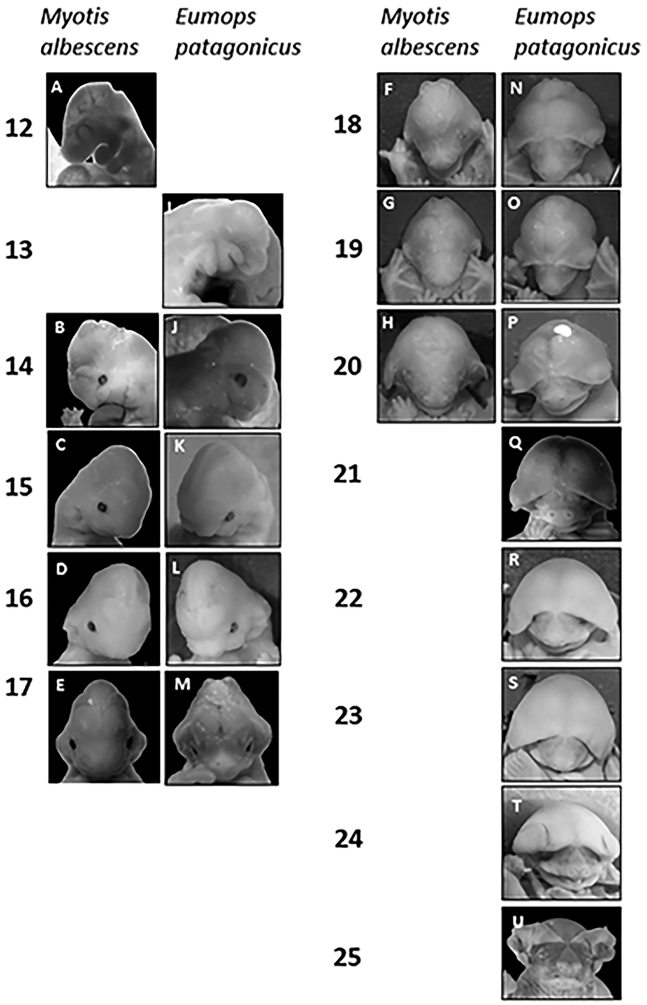

Fig. 9. *Myotis albescens* and *Eumops patagonicus* close-up of the craniofacial structures. (**A–H**) Craniofacial structure of *M. albescens*. (**I–U**) Craniofacial structure of *E. patagonicus.*

covers the middle of the tail. The autopodium of the forelimb is supported on the snout, covering the ocular region. The digit 1 (thumb) is free. The digits 2–5 are longer than in the previous stage and linked by the chiropatagium. The digits of the hindlimb are free and similar in length. The distal region of the tail is free.

Stage 19. CRL: 11.68 ± 0.70 mm (N = 3) (Fig. 7E–H). The embryo is opaque and whitish. The eyelids cover the eyes. The helix is more developed than in the previous stage and extends, covering the eyes completely. The tragus and antitragus are flat. The eyelids are closed. The propatagium and plagiopatagium are opaque and more developed than in the previous stages. The uropatagium is similar to in the previous stages. The stylopodium, zeugopodium, and phalanges of the forelimb and hindlimb are more developed than in the previous stages. The chiropatagium is opaque. The thumb of the forelimb and digits 1–5 of the hindlimb have a claw primordium. The external genitalia is not differentiated between the male and female yet; with distinguishable genital tubercle and prominences. The distal region of the tail is free.

Stage 20. CRL: 13.6 ± 0.41 mm (N = 2) (Fig. 7I–L). The embryo is opaque and whitish. The cephalic region is similar to in the previous stage. The tegument of the body has visible hair follicles. The autopodium of the forelimb covers the muzzle completely. The forelimb and the hindlimb are more developed than in the previous stage. The claws are cornified, and the calcaneus is visible. The tail is similar to in preceding stages.

Stage 21. CRL: 13.9 mm (N = 1) (Fig. 7M–P). The embryo is opaque and whitish. The helix is highly developed, forming two large expansions that cover the ocular region. The muzzle is well developed, and the flange of rhinarium is visible. The forelimb and hindlimb are more developed than in the previous stages. The autopodium of the forelimbs is crossed over the thoracic region below the muzzle. The autopodium of the hindlimb has a visible calcaneus and is more developed than in the previous stage. In the male, the penis is well developed and completely covered by the praeputium. The tail is similar to in the preceding stages.

Stage 22. CRL: 18.62 ± 0.64 mm (N = 3) (Fig. 8A–D). The helix is similar to in the previous stage. The eyelids are well developed and are not fused. The rhinarium is prominent, and the muzzle is more developed and with brown pigment spots in the maxillary region. The forelimb and the hindlimb are more developed than in the previous stage, and the claws are long. The trunk is well developed and white. The external genitals are well developed. The females are distinct, with vulva and clitoris. The male's penis is similar to in the previous stage. The tail is similar to in the previous stages.

Stage 23. CRL: 17.18 ± 0.69 mm (N = 3) (Fig. 8E–H). The muzzle is more pigmented than in the previous stage. The eyelid and rhinarium are more developed with pigments and dispersed points. The trunk is of light-brown coloration, with pigmentation dispersed in spots. The forelimb and hindlimb are similar to in the previous stage. The tail is similar to in the preceding stages, with pigmentation dispersed in spots.

Stage 24 (start of fetal stage). CRL: 20.13 ± 0.84 mm (N = 2) (Fig. 8I–L). In the head, the edge of the ears, eyelids, and rhinarium have more pigmentation, showing a dark-brown line. The incisors, canines and primordium premolars of the upper and lower jaws are visible as small elevations. The trunk has more color than in the previous stage. The wings are more developed, with dark regions on the humerus and thumb. The patagios are translucent. The hindlimb has colored fingers and ribbed claws. The genitalia is well developed and has strong pigmentation. The tail is more colored than in the previous stage.

Stage 25. CRL: 29.79 mm (N = 1) (Fig. 8M–P). In the head, the muzzle is well developed, and the vibrissae and hairs are visible in the upper and lower jaw. Pinna of the ear well develops, and the tragus and antitragus are similar to in adults. The eyelids are open. All the head and back have more pigmentation than in the previous stages. The wing does not have pigment in the membranes, but the hindlimb is completely colored. There is hair in the

hindlimb autopodium. The tail is more colored than in the previous stage.

DISCUSSION

In this article, we characterized the uterine morphology and the chorionic vesicle. We also identified the embryonic and fetal stages of *M. albescens* (Vespertilionidae) and *E. patagonicus* (Molossidae) based on the staging system proposed by Cretekos et al. (2005).

The Chiroptera exhibit a great morphological diversity as well as multiple reproductive specializations. Regarding this, a great anatomical and functional diversity of female reproductive tracts was described, mainly related to uterine morphology (Badwaik and Rasweiler, 2000). Depending on the degree of fusion of the uterine horns, the uterus might be duplex, bicornuate, or simple; these variants might occur even in the same family. In the Vespertilionidae family, Wimsatt (1979) described the "*Myotis* pattern," which is characterized by the bilateral ovarian function and the presence of a bicornuate uterus with gestational asymmetry. In *M. albescens*, the gestation occurs, in general, in the right horn (Myers, 1977), which coincides with our observations. In the Molossidae family, a bicornuate uterus with dextral dominance for *Chaerephon plicata* (Hood and Smith, 1983), *M. rufus* (Rasweiler, 1990), and *Tadarida brasiliensis* (Stephens, 1962) has been described, as well as a duplex uterus for *Mormopterus planiceps* (Crichton and Krutzsch, 1987). *E. patagonicus* has a bicornuate uterus with a dextral gestation, which coincides with the "Molossidae pattern" proposed by Wimsatt (1979).

Except *Myotis lucifugus* (Barbour and Davis, 1969), *M. adversus* (Dwyer, 1970), *M. daubentoni* (Kokurewicz and Bartmanska, 1992), *Nycticeius schlieffenii* (Van der Merwe and Rautenbach, 1988), *N. humeralis* (Bain and Humphrey, 1986), *Scotophilus heathi* (Madhavan, 1980), *S. dinganii*, *Pipistrellus nanus* (Happold and Happold, 1990), *Vespertilo superans* (Funakoshi and Uchida, 1981), *Tadarida pumila* (McWilliam, 1987), for which have been reported multiple births, most of the Chiroptera from Vespertilionidae and Molossidae family have a single parturition. This shows adaptive advantages for their livelihoods (Badwaik and Rasweiler, 2000). In this study, we observed a single embryo per uterus in both studied species, so we conclude that *M. albescens* and *E. patagonicus* are monotocous species.

In the order, there are many variants regarding the blastocyst implantation sites, the development of fetal membranes and placenta, characteristics of the interhaemal barrier, and the time of embryonic development (Badwaik and Rasweiler, 2000). The chorionic vesicle, in both studied species, showed similarities in the disposition of the extraembryonic membranes, but they differed in characteristics of the yolk sac and chorioallantoic placenta. In both analyzed species, the yolk sac membrane was well vascularized, although in *M. albescens* it was thin, translucent, and of a smooth surface, while in *E. patagonicus* it had thick walls, it was opaque and had a rough surface. *M. albescens* presented a well-developed discoid placenta with the caudal anti-mesometrial position from early gestation, coinciding with what has already been described for other families (Badwaik and Rasweiler, 2000). In *M. rufus* the chorioallantoic placenta (Rasweiler, 1990), until middle gestation, is diffuse and presents a placental disc. This placental disc grows, and it becomes the permanent placenta, while the diffuse villi regressed at the end of gestation. In *E. patagonicus*, unlike described for *M. rufus*, the diffuse placenta persist until the final stages of gestation (S. 24), which suggests that it functions as maternal–fetal exchange site, until final gestation.

Regarding the embryogenesis, in both studied species, early stages (S. 12, 13, and 14), middle stages (S. 15, 16, and 17) and late stages (S. 18, 19, 20, 21, 22, 23, and 24) were recognized. In the early stages, the embryonic morphology is similar between the two species analyzed in this study and those previously analyzed by other authors. In this stage, the main developmental events correspond to the body regionalization, cephalic structure organization, the formation of the primordium of the major organs and systems, and fore and hind limbs. The middle stage is characterized by the muzzle and pinna formation, fore and hind limb regionalization, and the formation of the patagium primordium. In the last stage, the overall growth of the embryo occurs; of its fore and hind limbs, patagium and the typical craniofacial features of each species are configured. Wang et al. (2010) compared the development of five species belonging to Vespertilionidae and Hipposideridae. They showed that the organogenic sequence of bats is uniform, but that there are differences, mainly in craniofacial structures. Also, in the species analyzed in this study, this occurred. In early stages of development, the embryonic morphology of *M. albescens* and *E. patagonicus* is similar, while in late stages (S. 18–24) differences are evident; mainly the craniofacial structures and uropatagium configuration—characteristics that allow their classification at the family level. In *M. albescens*, from S. 20, the tail is completely included in the uropatagium, and the pinna is small and pointed. In *E. patagonicus*, the tail is not included in the uropatagium, and the helix is developed and extended to the frontal region to merge with its counterpart on the opposite side. This characteristic is particular of the genus *Eumops.* Moreover, differences in time of fusion of maxillary and mandibular process were registered. In *M. albesces* (Fig. 9C,D), the maxillary and mandibular processes merge between S. 15 and S. 16. This also happens in *C. perspicillata* (Cretekos et al., 2005), *Pipistrellus abramus* (Tokita, 2006), *Miniopterus schreibersii fulginosus*, *Hipposideros armiger*, and *H. pratti* (Wang et al., 2010). In *E. patagonicus* (Fig.9L,M) and *M. rufus* (Nolte et al., 2009), the fusion of the maxillary processes occurs in S. 16, while the fusion of the mandibular processes occurs in S. 17. This difference in time of fusion of the maxillary and mandibular processes could be related to the morphology of the muzzle of each species, depending on their feeding habits. Nevertheless, we do not have enough information that allows us to hypothesize any answer about these variants.

Regarding the development of limbs and patagio, in both species, a similar morphogenetic pattern can be observed, except for the uropatagium, which in *M. albescens* is completely covering the tail. This is characteristic of each species.

When the morphogenesis of the limbs of different species of amniotes vertebrates is compared, differences are related to the timing of appearance of fore and hind limbs, as well as the rate of growth and development. In scaled reptiles such as *Calotes versicolor*

(Muthukkaruppan et al., 1970) and *Lacerta vivipara* (Dufaure and Hubert, 1961), both buds appeared at the same time and followed a similar sequence of development. In mammals such as *Ovis aries* (Bryden et al., 1972), *Felis cattus* (Illanes et al., 2007), and *Mus musculus* (Wanek et al., 1989) and birds such as *Gallus Gallus domesticus* (Hamburger and Hamilton, 1951), *Coturnix coturnix* (Ainsworth et al., 2010), *Columba livia* (Olea and Sandoval, 2012), and *Taeniopygia guttata* (Murray et al., 2013), it was described how the development of the forelimb bud appears before the hindlimb. This is similar to what has been reported for studied bats species. The forelimbs and hindlimbs of bats are unique among mammals and therefore ideal candidates for comparative studies. Comparative studies of limb development carried out in *Miniopterus natalensis* and *Mus musculus* by Hockman et al. (2009) demonstrated morphological differences starting from the embryonic middle stage. They conclude that bats follow a particular morphogenetic model characterized by a fast growing of fingers and the forelimb zeugopodium. If we compare the forelimb development in the early stages with other mammal embryos, there are many similarities in the formation of the digital plate, but in bats, this membrane never disappears. The development of the forelimbs in bats changes in the middle and late stages, because there is a big growth at this stage. The length of the time of development of forelimbs makes bats a great model for comparative studies, like a model of heterochrony, because changes in the developmental timing (heterochrony) are considered to be important in producing morphological change during evolution (Gould, 1977). We have seen that the growth of wings in both species was similar, and that might be related to the fact that both have similar flights habits.

Gould (1977), McNamara (1997) and Hall (1998) suggest that the adult's morphology is the result of a series of complex processes that occur during embryonic development, and that morphological diversity is explained by modifications in ancestral development patterns. This emphasizes the importance of analyzing and describing the morphogenetic events in different vertebrate species such as bats. This article is the first contribution to the knowledge of embryogenesis of Argentinian bats, and it serves as a basis for future comparisons with other species.

ACKNOWLEDGMENTS

We would like to thank Ph.D. Francisca Milano and Lic. Carlos González for their donation of the study material. We would also like to make a special acknowledgment of Stephen Geil Devincenzi for his help with the English language. This study was supported by PI: F12 008 of Secretaria General de Ciencia y Técnica de la Universidad Nacional del Nordeste.

LITERATURE CITED

Adams RA. 1992. Stages of development and sequence of bone formation in the little brown bat, *Myotis lucifugus*. J Mammal 73:160–167.

Ainsworth SJ, Stanley RL, Evans DJ. 2010. Developmental stages of the Japanese quail. J Anat 216(1):3–15.

Badwaik NK, Rasweiler JJ IV. 2000. Pregnancy. In: Crichton EG, Krutzsch PH, editors. *Reproductive biology of bats*. London: Academic Press. p 201–281.

Bain JR, Humphrey SR. 1986. Social organization and biased primary sex ratio of the evening bat, *Nycticeius humeralis*. Florida Sci 49:22–31.

Barbour RW, Davis WH. 1969. *Bats of America*. Lexington: The University Press of Kentucky. p 286.

Barquez RM, Mares AM, Braun JK. 1999. *The bats of Argentina*. Lubbock, TX: Museum of Texas Tech University p. 90–90, 203–207.

Bryden MM, Evans HE, Binns W. 1972. Embryology of the sheep. I. Extraembryonic membranes and the development of body form. J Morphol 138(2):169–185.

Cretekos CJ, Weatherbee SD, Chen CH, Badwaik NK, Niswander L, Behringer RR, Rasweiler JJ IV. 2005. Embryonic staging system for the short-tailed fruit bat, *Carollia perspicillata*, a model organism for the mammalian order Chiroptera, based upon timed pregnancies in captive-bred animals. Dev Dyn 233:721–738.

Crichton EG, Krutzsch PH. 1987. Reproductive biology of the female little mastiff bat, *Mormopterus planiceps* (Chiroptera: Molossidae) in southeast Australia. Am J Anat 178:369–386.

Dufaure JP, Hubert J. 1961. Table de developpement du lezard vivipare: *Lacerta* (*Zootoca*) *vivipara* Jacquin. Arch Anat Microsc Morphol Exp 50(3):309.

Dunham AE. 1983. In: Huey RD, Pianka ER, Schoener TW, editors. *Realized niche overlap, resource abundance, and intensity of interspecific competition, Lizard ecology*. Harvard, Univ Pres. Cambridge, Massachusetts. E.E.U.U. p 261–280.

Dwyer PD. 1970. Latitude and breeding season in a polyestrous species of *Myotis adversus*. J Mammal 51:405–410.

Gould SJ. 1977. *Ontogeny and phylogeny*. Harvard University Press, Cambridge, Massachusetts. E.E.U.U.

Funakoshi K, Uchida TA. 1981. Feeding activity during the breeding season and postnatal growth in the Namie's frosted bat, *Vespertilio superans superans*. Jpn J Ecol 31:66–77.

Hall BK. 1998. *Evolutionary developmental biology*. 2nd ed. New York: Chapman & Hall.

Hamburger V, Hamilton HL. 1951. A series of normal stages in the development of the chick embryo. J Morphol 88:49–92.

Happold DCD, Happold M. 1990. The domiciles, reproduction, social organization and sex ratios of *Pipistrellus nanus* (Vespertilionidae. Chiroptera) in Malawi, Central Africa. Z Siiugetierk 55:145–160.

Hockman D, Mason MK, Jacobs DS, Illing N. 2009. The role of early development in mammalian limb diversification: A descriptive comparison of early limb development between the natal long-fingered bat (Miniopterus natalensis) and the mouse (Mus musculus). Developmental Dynamics. 238(4):965–979.

Hood CS, Smith JD. 1983. Histomorphology of the female reproductive tract in Phyllostomid bats. Occ Pap Mus Texas Tech Univ 86:1–38.

Illanes J, Orellana C, Fertilio B, Leyton V, Venegas F. 2007. Análisis macroscópico y microscópico del desarrollo embrionario y fetal en el gato (*Felis catus*), en relación con el desarrollo de la vesícula coriónica y de la placenta. Int J Morphol 25(3):467–481.

Jones KE, Purvis A, MacLarlon A, ORP B–E, Simons NB. 2002. A phylogenetic supertree of the bats (Mammalia: Chiroptera). Biol Rev 77(2):223–259.

Kokurewicz T, Bartmanska J. 1992. Early sexual maturity in male Daubenton's bats *Myotis daubentoni* (Kuhl, 1819) (Chiroptera: Vespertilionidae); field observations and histological studies on the genitalia. Myotis 30:95–107.

Madhavan A. 1980. Breeding habits and associated phenomena in some Indian bats. Part VI. Scotophilus heathi (Horsefield)-Vespertilionidae. J Bombay Nat Hist Soc 77:227–237.

McNamara KJ. 1997. *Shapes of time: the evolution of growth and development*. Baltimore: Johns Hopkins University Press.

McWilliam A. 1987. In: Fenton MB, Racey PA, Rayner JMV, editors. *The reproductive and social biology of* Coleura afra *in a seasonal environment, Recent advances in the study of bats*. Cambridge: Cambridge University Press. p 324–350.

Miller-Butterworth CM, Murphy WJ, SJ O`B, Jacobs DS, Springer MS, Teeling EC. 2007. A family matter: conclusive resolution of the taxonomic position of the long-fingered bats, *Miniopterus*. Mol Biol Evol 24(7):1553–1561.

Murray JR, Varian Ramos CW, Welch ZS, Saha MS. 2013. Embryological staging of the Zebra Finch, *Taeniopygia guttata*. J Morphol 274(10):1090–1110.

Muthukkaruppan VR, Kanakambika P, Manickavel V, Veeraraghavan K. 1970. Analysis of the development of the lizard, *Calotes versicolor*. I. A series of normal stages in the embryonic development. J Morphol 130(4):479–489.

Myers P. 1977. Patterns of reproduction of four species of vespertilionid bats in Paraguay. Univ Calif Publ Zool 107:1–41.

Nolte MJ, Hockman D, Cretekos CJ, Behringer RR, Rasweiler JJ IV. 2009. Embryonic staging system for the black mastiff bat, *Molossus rufus* (Molossidae), correlated with structure–function relationships in the adult. Anat Rec 292:155–178.

Nowak RM. 1999. *Walker's mammals of the world*. 6th ed. Baltimore: The Johns Hopkins University Press.

Olea GB, Sandoval MT. 2012. Embryonic development of *Columba livia* (Aves: Columbiformes) from an altricial–precocial perspective. Rev Colomb Cienc Pec 25(1):3–13.

Rasweiler JJIV. 1990. Implantation, development of the fetal membranes and placentation in the captive black mastiff bat *Molossus ater*. Am J Anat 187:109–136.

Schumacher S. 1932. Die Entwicklung der Fledermausflugh-aut. Zeitschr Anat Entwickl 98:703–721.

Sikes RS; Animal Care and Use Committee of the American Society of Mammalogists. 2016. 2016 Guidelines of the American Society of Mammalogists for the use of wild mammals in research and education. Journal of Mammalogy. 97(3), 663–688.

Stephens RJ. 1962. Histology and histochemistry of the placenta and fetal membranes in the bat, *Tadarida brasiliensis cynocephala* (with notes on maintaining pregnant bats in captivity). Am J Anat 111:259–286.

Teeling EC, Springer MS, Madsen O, Bates P, O`Brien SJ, Murphy WJ. 2005. A molecular phylogeny for bats illuminates biogeography and the fossil record. Science 307:580–584.

Tokita M. 2006. Normal embryonic development of the Japanese pipistrelle, *Pipistrellus abramus*. Fortschr Zool 109:137–147.

Van der Merwe NJ, Rautenbach IL. 1988. The placenta and foetal membranes of the lesser yellow house bat, *Scotophilus borbonicus* (E. Geoffroy, 1803) (Chiroptera: Vespertilionidae). S Afr J Zool 23: 320–327.

Wanek N, Muneoka K, Holler-Dinsmore G, Burton R, Bryant SV. 1989. A staging system for mouse limb development. J Exp Zool 249:41–49.

Wang Z, Han N, Racey PA, Ru B, He G. 2010. A comparative study of prenatal development in *Miniopterus schreibersii fuliginosus*, *Hipposideros armiger* and *H. pratti*. BMC Dev Biol 10(1):1–17.

Wilson DW, Reeder DM. 2005. Introduction. In: Wilson DE, Reeder DA, editors. *Mammalian species of the world. A taxonomic and geographic reference*, Vol. 1. 3rd ed. Baltimore: John Hopkins University Press. p xxv–xxix.

Wimsatt WA. 1979. Reproductive asymmetry and unilateral pregnancy in Chiroptera. J Reprod Fertil 56:345–357.